

Poteri e contrattazione: professioni tecniche tra Stato e Città nel Piemonte sabauda

*Original*

Poteri e contrattazione: professioni tecniche tra Stato e Città nel Piemonte sabauda / Gianasso, E., Cattaneo, M.. - ELETTRONICO. - 1:(2023), pp. 316-317. (Adaptive cities through postpandemic lens. Ripensare tempi e sfide della città flessibile. Times and Challenges in Urban history. Torino 06/09/2022 - 10/09/2022).

*Availability:*

This version is available at: 11583/2986651 since: 2024-03-07T16:47:38Z

*Publisher:*

AISU International

*Published*

DOI:

*Terms of use:*

This article is made available under terms and conditions as specified in the corresponding bibliographic description in the repository

*Publisher copyright*

(Article begins on next page)



# Measurement of the cosmic charged particle rate at sea level in the latitude range $35^\circ \div 82^\circ$ N with the PolarquEEEst experiment

M. Abbrescia<sup>1,2</sup>, C. Avanzini<sup>3,4</sup>, L. Baldini<sup>3,4</sup>, R. Baldini Ferroli<sup>5</sup>, G. Batignani<sup>3,4</sup>, M. Battaglieri<sup>6</sup>, S. Boi<sup>7,8</sup>, E. Bossini<sup>3,4</sup>, F. Carnesecchi<sup>9</sup>, D. Cavazza<sup>10</sup>, C. Cicalò<sup>8</sup>, L. Cifarelli<sup>10,11</sup>, F. Coccetti<sup>12</sup>, E. Coccia<sup>13</sup>, A. Corvaglia<sup>14</sup>, D. De Gruttola<sup>15,16</sup>, S. De Pasquale<sup>15,16</sup>, L. Galante<sup>17</sup>, M. Garbini<sup>10,12</sup>, G. Gemme<sup>6,12</sup>, I. Gnesi<sup>12,18</sup>, E. Gramstad<sup>19</sup>, S. Grazi<sup>6,20</sup>, E. S. Håland<sup>19</sup>, D. Hatzifotiadou<sup>9,10</sup>, P. La Rocca<sup>21,22</sup>, Z. Liu<sup>23</sup>, L. Lombardo<sup>24</sup>, G. Mandaglio<sup>20,22</sup>, A. Margotti<sup>10</sup>, G. Maron<sup>25</sup>, M. N. Mazziotta<sup>2,a</sup>, A. Mulliri<sup>7,8</sup>, R. Nania<sup>10</sup>, F. Noferini<sup>10,b</sup>, F. Nozzoli<sup>26</sup>, F. Ould-Saada<sup>19</sup>, F. Palmonari<sup>10,11</sup>, M. Panareo<sup>14,27</sup>, M. P. Panetta<sup>14</sup>, R. Paoletti<sup>3,28</sup>, M. Parvis<sup>24</sup>, C. Pellegrino<sup>29</sup>, L. Perasso<sup>6</sup>, O. Pinazza<sup>10</sup>, C. Pinto<sup>30</sup>, S. Pisano<sup>5,12</sup>, F. Riggi<sup>21,22</sup>, G. Righini<sup>31</sup>, C. Ripoli<sup>15,16</sup>, M. Rizzi<sup>2</sup>, G. Sartorelli<sup>10,11</sup>, E. Scapparone<sup>10</sup>, M. Schioppa<sup>18,32</sup>, G. Scioli<sup>10,11</sup>, A. Scribano<sup>3,28</sup>, M. Selvi<sup>10</sup>, M. Taiuti<sup>6,33</sup>, G. Terreni<sup>3</sup>, A. Trifirò<sup>20,22</sup>, M. Trimarchi<sup>20,22</sup>, C. Vistoli<sup>29</sup>, L. Votano<sup>34</sup>, M. C. S. Williams<sup>9,23</sup>, A. Zichichi<sup>9,10,11,12,23</sup>, R. Zuyewski<sup>9,23</sup>

<sup>1</sup> Dipartimento di Fisica “M. Merlin” dell’Università e del Politecnico di Bari, via Amendola 173, 70125 Bari, Italy

<sup>2</sup> INFN, Sezione di Bari, via Orabona 4, 70126 Bari, Italy

<sup>3</sup> INFN, Sezione di Pisa, largo Bruno Pontecorvo 3, 56127 Pisa, Italy

<sup>4</sup> Dipartimento di Fisica “E. Fermi”, Università di Pisa, largo Bruno Pontecorvo 3, 56127 Pisa, Italy

<sup>5</sup> INFN, Laboratori Nazionali di Frascati, via Enrico Fermi 54, 00044 Frascati, RM, Italy

<sup>6</sup> INFN, Sezione di Genova, via Dodecaneso, 33, 16146 Genoa, Italy

<sup>7</sup> Dipartimento di Fisica, Università di Cagliari, S.P. Monserrato-Sestu Km 0,700, 09042 Monserrato, CA, Italy

<sup>8</sup> INFN, Sezione di Cagliari, Complesso Universitario di Monserrato, S.P. per Sestu, Km 0, 700, 09042 Monserrato, CA, Italy

<sup>9</sup> CERN, Esplanade des Particules 1, 1211 Geneva 23, Switzerland

<sup>10</sup> INFN, Sezione di Bologna,

viale Carlo Berti Pichat 6/2, 40127 Bologna, Italy

<sup>11</sup> Dipartimento di Fisica e Astronomia “A. Righi”, Università di Bologna, viale Carlo Berti Pichat 6/2, 40127 Bologna, Italy

<sup>12</sup> Museo storico della Fisica e Centro studi e ricerche “E. Fermi”, via Panisperna 89/a, 00184 Rome, Italy

<sup>13</sup> Gran Sasso Science Institute, viale Francesco Crispi 7, 67100 L’Aquila, Italy

<sup>14</sup> INFN, Sezione di Lecce, via per Arnesano, 73100 Lecce, Italy

<sup>15</sup> Dipartimento di Fisica “E. R. Caianiello”, Università di Salerno, via Giovanni Paolo II, 132, 84084 Fisciano, SA, Italy

<sup>16</sup> INFN, Gruppo Collegato di Salerno, Complesso Universitario di Monte S. Angelo, ed. 6 via Cintia, 80126 Naples, Italy

<sup>17</sup> Teaching and Language Lab (tllab), Politecnico di Torino, corso Duca degli Abruzzi 24, Turin, Italy

<sup>18</sup> INFN, Gruppo Collegato di Cosenza, via Pietro Bucci, Rende, Cosenza, Italy

<sup>19</sup> Physics Department, Oslo University, P.O.Box 1048, 0316 Oslo, Norway

<sup>20</sup> Dipartimento di Scienze Matematiche e Informatiche, Scienze Fisiche e Scienze della Terra, Università di Messina, viale Ferdinando Stagno d’Alcontres 31, 98166 Messina, ME, Italy

<sup>21</sup> Dipartimento di Fisica e Astronomia “E. Majorana”, Università di Catania, via S. Sofia 64, 95123 Catania, Italy

<sup>22</sup> INFN, Sezione di Catania, via S. Sofia 64, 95123 Catania, Italy

<sup>23</sup> ICSC World laboratory, Geneva, Switzerland

<sup>24</sup> Dipartimento di Elettronica e Telecomunicazioni Politecnico di Torino, corso Duca degli Abruzzi 24, Turin, Italy

<sup>25</sup> INFN, Laboratori Nazionali di Legnaro, viale dell’Università 2, 35020 Legnaro, Italy

<sup>26</sup> INFN, Trento Institute for Fundamental Physics and Applications, via Sommarive, 14, 38123 Povo, TN, Italy

<sup>27</sup> Dipartimento di Matematica e Fisica “E. De Giorgi”, Università del Salento, via per Arnesano, 73100 Lecce, Italy

<sup>28</sup> Dipartimento di Scienze Fisiche, della Terra e dell’Ambiente, Università di Siena, via Roma 56, 53100 Siena, Italy

<sup>29</sup> INFN-CNAF, viale Carlo Berti Pichat 6/2, 40127 Bologna, Italy

<sup>30</sup> Physik Department, Technische Universität München, James-Frank-Straße 1, 85748 Garching bei, Munich, Germany

<sup>31</sup> CNR, Istituto di Fisica Applicata “Nello Carrara”, via Madonna del Piano 10, 50019 Sesto Fiorentino, FI, Italy

<sup>32</sup> Dipartimento di Fisica, Università della Calabria, via Pietro Bucci, Rende, CS, Italy

<sup>33</sup> Dipartimento di Fisica, Università di Genova, via Dodecaneso, 33, 16146 Genoa, GE, Italy

<sup>34</sup> INFN, Laboratori Nazionali del Gran Sasso, via G. Acitelli 22, 67100 Assergi, AQ, Italy

Received: 7 July 2022 / Accepted: 24 February 2023

© The Author(s) 2023

**Abstract** After its successful campaign of measurements beyond the Polar Arctic Circle, the PolarquEEEst experiment measured the cosmic charged particle rate at sea level in a latitude interval between  $35^\circ$  N and  $82^\circ$  N. In this paper, these measurements are described and the corresponding results are discussed.

## 1 Introduction

The PolarquEEEst experiment recently measured, with an unprecedented precision, better than  $\pm 1\%$ , that the cosmic charged particle rate at sea level stays constant in the latitude range between  $66^\circ$  N and  $82^\circ$  N [1]. Due to the Earth geomagnetic field and its roughly di-polar nature, this rate is expected to be modulated with latitude, with an increase from the equatorial regions until a flattening appears at around  $50^\circ$  latitude.

Relatively few measurements exist, that experimentally check this prediction. The earliest compilation of the available measurements was done by Compton [2], where also a comparison with the first Lemaître–Vallarta model is reported [3]. However, these data came from multiple campaigns of measurements and, although they asserted the increase with latitude of the charged cosmic ray rate, they were affected by rather significant uncertainties.

The PolarquEEEst detector was originally designed to be hosted on a small sailboat, and is therefore relatively small, light-weighted and easy to be carried around also by car. This allowed to perform, in 2018 and 2019, a series of measurements of the cosmic charged particle rate across Europe over a latitude range going from  $35.5^\circ$  N, corresponding to the Lampedusa island in Italy, to the city of Hannover, in Germany, at  $52.3^\circ$  N. The added value of these measurements derives from the fact that they were performed with the very same detector transported at various locations, allowing a much better knowledge of the systematic errors with respect to the previously mentioned results, derived from a compilation of several data from multiple different devices.

Very few other measurements are available, which were collected using the same detector moved to different locations, like the one performed up to the Chutkoski peninsula ( $\approx 66^\circ$  N) [4], along the Siberian eastern coast, however obtained with neutrons. See also [5] for a survey of the available data. Recently the TRISTAN collaboration presented some results on the cosmic charged particle rate using resistive plate chambers (RPCs) installed on board of an oceanographic ship travelling from Vigo (Spain) to Punta Arenas (Chile) [6]. Also the POLASTERN project, performed in collaboration with DESY and using scintillation counters, col-

lected data during several years from the North to the South Pole [7]. From the published data it is however difficult to derive the appropriate corrections and/or normalisation factors that would allow a straightforward comparison among them. This is why no comparison with the results presented here will be attempted.

In this paper, a brief description of the PolarquEEEst detector is reported in Sect. 2. The data taking campaign with the corrections applied to the data and the systematic uncertainties are discussed in Sects. 3 and 4, respectively. Then predictions on the cosmic particle rate as a function of the latitude, obtained using the PARMA model [8,9], widely used in this field, are presented in Sect. 5. Finally the results obtained are reported with few remarks in Sect. 6.

## 2 The PolarquEEEst detectors

The PolarquEEEst experiment is part of the Extreme Energy Events (EEE) project, sponsored by the Museo Storico della Fisica e Centro Studi e Ricerche Enrico Fermi [10,11] and the Istituto Nazionale di Fisica Nucleare (INFN) in Italy. It is a unique example of an experiment on cosmic rays that includes an important component of scientific educational dissemination to high school students. The measurements described herein were performed with a detector conventionally called POLA-01, one of three identical devices built for this experiment. The other two, called POLA-02 and POLA-03, were permanently located inside two high school institutes: one at Nesodden, close to Oslo in Norway, at  $59.84^\circ$  N,  $10.68^\circ$  E and 84 m of altitude, and the other at Bra, in Piedmont (Italy), at  $44.69^\circ$  N,  $7.86^\circ$  E and 310 m of altitude. Both have been used to monitor cosmic particle rate seasonal variations and correct the data accordingly, as discussed below.

A PolarquEEEst detector consists of two planes of 1 cm thick scintillators, each divided into four equal tiles of  $20 \times 30 \text{ cm}^2$ . Each tile is wrapped with a mylar foil and four of them are inserted individually in a closed DELRIN dark box to define a plane. The two planes are then placed inside a bigger DELRIN box with the readout electronics placed outside. Readout is performed by means of silicon photomultipliers (SiPMs), two per tile, positioned at opposite corners. Front-end boards amplify and discriminate the analog signals, shaping them also into Low Voltage Differential (LVD) signals, whose time-over-threshold amplitude is used to estimate the signal charge. Data are collected via TDCs hosted on a custom readout board, after a trigger is defined by the coincidence of signals from at least three SiPMs, two from the same tile of a plane (either top or bottom), the third from a tile in the other plane. Time stamp and detector position are obtained through GPS signals. Also other important parameters, like temperature, pressure and inclination/orientation are measured by means of suitable sensors, and recorded

<sup>a</sup> e-mail: [Marionicola.Mazziotta@ba.infn.it](mailto:Marionicola.Mazziotta@ba.infn.it) (corresponding author)

<sup>b</sup> e-mail: [francesco.noferini@bo.infn.it](mailto:francesco.noferini@bo.infn.it) (corresponding author)

**Table 1** List of the locations where POLA-01 took data

Location	Period (day/month/year)	Latitude (°)	Altitude (m)
<i>CERN (Geneva)</i>	26/06/18–28/06/18	46.23	441
<i>Nanuq</i>	21/07/18–05/09/18	66.82	0
<i>Vigna di Valle</i>	27/11/18	42.1	153
<i>Cosenza</i>	04/12/18–05/12/18	39.3	222
<i>Cefalù</i>	06/12/18	38.0	0
<i>Catania</i>	31/01/19	37.5	158
<i>Lampedusa*</i>	07/03/19–08/03/19	35.5	10
<i>Bologna</i>	08/04/19	44.5	81
<i>Bologna-Hannover</i>	10/04/19	44.6–51.0	200–700
<i>Hannover-Frankfurt</i>	11/04/19	52.3	60
<i>Frankfurt-Geneva</i>	12/04/19	50.0–46.0	100–500

The island of Lampedusa was reached from Sicily by ferry boat; measurements were only performed on the island

to be used later on during the analysis process. Data were sent to the INFN CNAF computer centre to be reconstructed and stored. More details on the PolarquEEEst experiment, its detectors, and its first data taking campaign are available in [1].

Since the PolarquEEEst experiment was conceived within the same philosophy of EEE, namely as a high level scientific programme but also as an outreach initiative for high school students, detector construction and daily detector monitoring were performed by high school students.

### 3 Data taking at different latitudes and corrections

The data presented in this paper were collected in two phases. The POLA-01 detector was initially installed on board of the 60-feet eco-friendly sailboat *Nanuq*, which from July till August 2018 travelled from Ísafjörður (Iceland), reached Longyearbyen (Svalbard, Norway), then circumnavigated the Svalbard archipelago reaching the maximum latitude of 82°07' N, and ended its trip on September 4, in Tromsø (Norway). This sailing cruise was part of the Polarquest2018 expedition [12], and the data collected have been already analysed [1].

Then, in the Fall 2018 until the first months of 2019, the POLA-01 detector was transported “on the road” in a trip by car, featuring many stops in Italy and Germany as summarized in Table 1, which reports the latitude, the altitude and the geographical names of the locations where the data were collected. A map of the overall trip of the POLA-01 detector is visualised in Fig. 1. During the trip, data were taken in time slots typically of few hours per location, except in some cases, like in Catania and Lampedusa, where the data taking lasted a couple of days. In the meantime, the POLA-02 and POLA-03 detectors almost continuously took data at

their permanent locations cited above, in Piedmont (Italy) and Norway.

In order to derive the effect of latitude on the measured charged particle rates, other sources of possible rate variations had to be estimated and accurately subtracted.

All data were first corrected for the barometric effect, consisting of an anti-correlation between atmospheric pressure and the measured cosmic particle rate, due to the fact that higher atmospheric pressure values imply an increased absorption of secondary particles by the atmosphere. In Fig. 2 the POLA-01 rate is plotted as a function of the atmospheric pressure. The barometric coefficient was obtained as coefficient of an exponential fit to the data. Similar plots and fits were done for POLA-02 and POLA-03. Data taken at a given pressure were thus corrected by dividing by the fit function  $\exp(-b(P - P_0))$ , where  $b = 2.24 \pm 0.01 \times 10^{-3} \text{ mbar}^{-1}$  is the barometric coefficient derived from the fit,  $P$  the pressure and  $P_0$  a reference value set to 1011.88 mbar as in [1].

Data collected by the POLA-01 detector during its trip in Italy and Germany were sometimes taken at different altitudes. No specific correction has been applied regarding altitude, apart from the fact that, in general, data collected at higher altitude were also usually collected at a lower atmospheric pressure, which was corrected as described above. The effect of altitude has been accounted for as a systematic error of the measured rates, and is evaluated in Sect. 4.

Data collected on board the *Nanuq* sailing boat by POLA-01 were also corrected for the boat inclination. The correlation between the measured rate and the inclination angle of the boat with respect to the vertical, measured by the accelerometer sensors of the detector (see Sect. 2), is shown in Fig. 3. The data are fitted with the function  $(1 - a(1 - \cos \theta))$  where  $\theta$  is the zenith angle and  $a = 1.31 \pm 0.02$  the parameter derived from the fit. Also in this case, the correction was applied by dividing the rate by the fitted function.

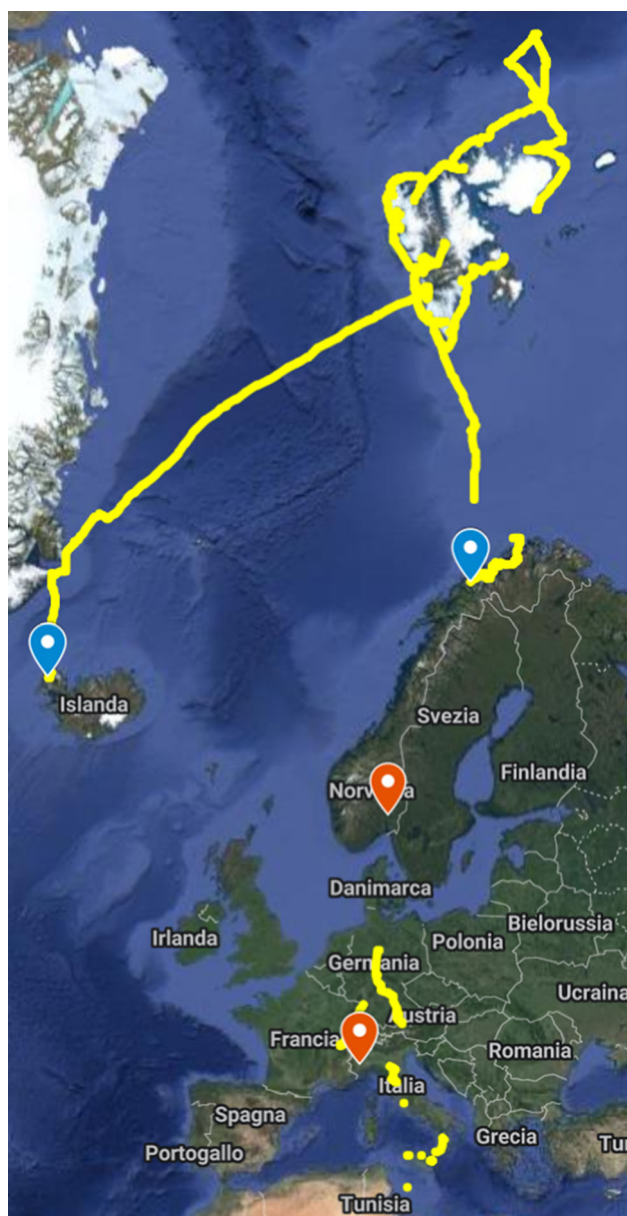


**Fig. 1** The trip of POLA-01 (yellow line) as traced by the GPS system. The sites of Ísafjörður (Iceland) and Tromsø (Norway), which were the start and end points of the Nanuq sailing cruise around the Svalbard, are shown with blue markers. The sites of Nesodden (Norway) and Bra (Italy), where the reference detectors POLA-02 and POLA-03 were located, are also shown with red markers

More details on both pressure and inclination correction procedures are thoroughly described in [1] where, however, the gyroscopic information was instead used.

Finally, concerning POLA-01 also an efficiency correction ( $\varepsilon = 96\%$ ) was used. The value of the efficiency was measured at CERN at the end of the whole expedition using as external reference detector one of the EEE muon-tracking telescopes.

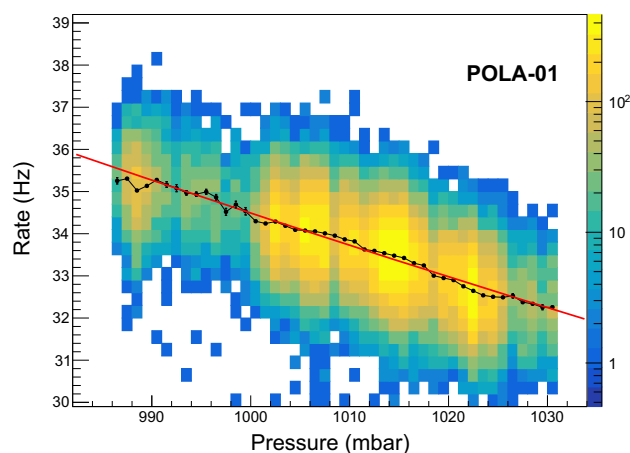


**Fig. 2** Cosmic particle rate measured by POLA-01 as a function of atmospheric pressure. An exponential fit, in red, is superimposed to the data (see text)

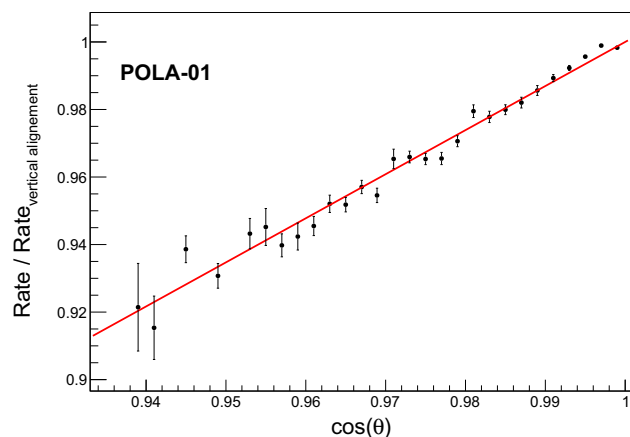


**Fig. 3** Correlation between the cosmic particle rate measured by the POLA-01 detector on board of the sailboat Nanuq and its inclination with respect to the vertical. A linear fit, in red, is superimposed to the data

As for POLA-02 and POLA-03, the two reference detectors permanently located inside school buildings are subject to further corrections. The presence of structures above and around the detectors, such as walls and ceilings, reduces the measured cosmic particle rate. Dedicated data, collected by moving the detectors outside the buildings hosting them, were used to correct for this effect. The ratios between the rates measured during these dedicated data taking periods, indoor and outdoor, are shown in Fig. 4. While for POLA-02 the rate reduction indoor is of the order of 4%, for POLA-03 this is much higher and around 22%, due to a much thicker building structure present above it.

The data used in the present analysis were taken over several months, so it was also necessary to consider a seasonal rate variation, related to the varying solar activity. This was estimated by using the two reference detectors POLA-02 and POLA-03, whose rates as a function of time, after pressure

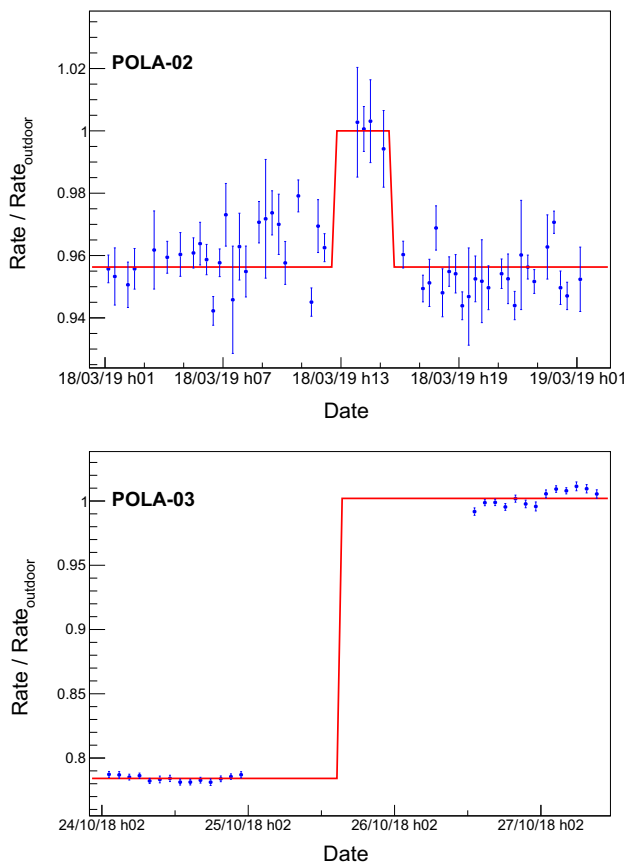


**Fig. 4** Ratios of the measured rates, indoor and outdoor, for the POLA-02 (upper panel) and POLA-03 (lower panel) detectors

and building structure corrections, are shown in Fig. 5 for a period of about one year, from July 21, 2018 to August 31, 2019. Since data were collected by POLA-02 and POLA-03 at two different latitudes, POLA-03 rate was increased by 1% in order to be superimposed to POLA-02 rate in Fig. 5. In both detectors, the rate was measured to be changing in time, with a modulation of  $\pm 1.8\%$ , and a broad maximum in mid January 2019 and minima during Summer 2018 and 2019. This seasonal effect was observed in the past from other muon telescopes with a similar energy threshold [13], and our results are compatible with what previously found. Therefore, POLA-01 data were accordingly divided by the reported modulation depending on the date.

Finally it should be recalled that, although the longitudinal coordinates of the various measurements are slightly different, the related corrections are negligible and inside the reported errors.

#### 4 Systematic uncertainties

Systematic uncertainties were estimated by varying the assumptions used in the calculation of the corrections and on the environment conditions.

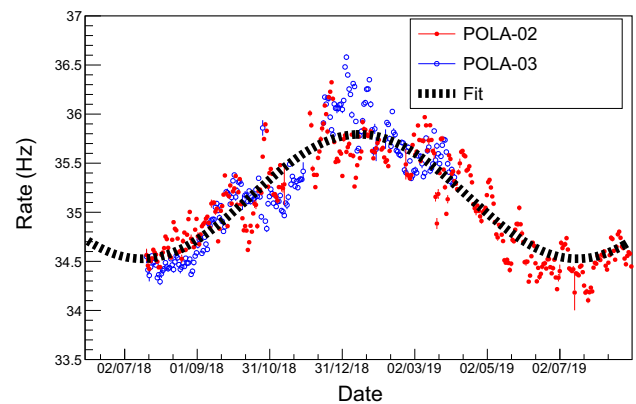


**Fig. 5** POLA-02 and POLA-03 ( $\times 1.01$ ) measured cosmic particle rate as a function of time, for the period from July 7, 2018 to August 31, 2019. A fit to the data, after normalisation, is superimposed

The barometric coefficient used to correct for pressure effect was varied by  $\pm 10\%$  and the maximal difference with respect the default value was taken as uncertainty. This resulted in a relative error on the measured rate of 0.5%.

Since some measurements were not collected at sea level (the maximum altitude reached was around 700 m) a dedicated study was performed by collecting data from 0 to 2000 m on the slopes of the Etna Volcano close to Catania. Such a study showed a significant altitude effect (1.4%) which was not re-absorbed by pressure correction above 1 km. Below 1000 m the effect was estimated to be 0.2%.

The linear coefficient of the detector inclination/orientation correction was varied by  $\pm 10\%$  and no relevant differences were found.

The parameterisation of the seasonal effect was varied by changing the amplitude of the modulation by  $\pm 10\%$  and the position of the winter peak by  $\pm 1$  week. The associated relative uncertainty on the rate was estimated to be at the level of 0.2%.

For the measurements above  $60^\circ$  of latitude, where a constant rate is expected, a 0.5% daily fluctuation was observed. Such a fluctuation was assigned as a systematic uncertainty for external conditions (e.g. solar activity).

The stability of the efficiency along the full period was checked by comparing the rates measured independently by the 4 pairs of vertically aligned scintillator counters from the two superimposed planes of the PolarquEEEst detector. In fact, each detector plane is segmented in 4 tiles. From each pair of tiles in vertical correspondence it is possible to measure an independent rate. Such a comparison is particularly useful since the 4 pairs are expected to measure the same rate independently of any external condition (pressure, seasonal effect, etc.). The consistency of the 4 rates was checked and their differences were assigned as systematic uncertainties. These were found to be in the range 0.4–0.7%.

Note that an extra systematic contribution was included for the measurements made on the road, due to the fact that the detector and electronics were positioned upside down inside the car used for transportation, hence a different material budget had to be accounted for. Such an additional error contribution does not apply to the measurements at the Svalbard and, in Italy, at Cosenza and Lampedusa.

In Table 2 a summary of the above estimates is reported. The total uncertainty was calculated by summing the squares of all contributions.

### 5 Model expectations

In order to have an estimate of the presumable behaviour of the measured cosmic rate vs. latitude, the C++ Version 4.10 of PARMA (PHITS-based Analytical Radiation Model in the Atmosphere) was used.<sup>1</sup> This software models the results obtained by a sophisticated extensive air shower (EAS) simulation, with the goal of estimating the cosmic ray flux in a wide variety of conditions. The PARMA model is validated using the results of the EAS simulation, as well as multiple sets of experimental data relative to different particles obtained in various momentum ranges under various conditions and its results are used in research areas such as geosciences, cosmic ray physics, and radiation research [8,9]. Note however that the used reference data are above few hundred MeV.

The differential vertical cosmic ray flux, in unit of particles/(MeV s cm<sup>2</sup> sr), computed using the PARMA code, for a point on the Earth at sea level, with coordinates 40° N and 15° E, for the day August 1, 2018, is shown in Fig. 6. Here, the various contributions coming from  $\mu^\pm$ ,  $e^\pm$ ,  $p$ ,  $n$  and  $\gamma$  are indicated separately. As expected, the contributions coming from  $\mu^\pm$  (the two charges being almost completely superimposed in the figure) dominate at energies larger than few hundred MeV, while at lower energies neutral particles like photons and neutrons are the most abundant.

The expected cosmic particle rate was evaluated by folding the differential vertical flux with the PolarquEEEst detector acceptance, and assuming a  $\cos^2\theta$  angular distribution (where  $\theta$  is the zenith angle) for secondary cosmic rays at sea level [14]. The detector acceptance was computed simulating an isotropic and uniform distribution of downward tracks within a sphere of radius  $R_{sph}$ , with a fluency equal to  $1/\pi R_{sph}^2$ , and then selecting only those tracks traversing one top and one bottom detector tiles, with a corresponding energy loss larger than 1 MeV. For this simulation, the FLUKA code was used [15,16], and different particle types with a uniform distribution in logarithm of the energy were

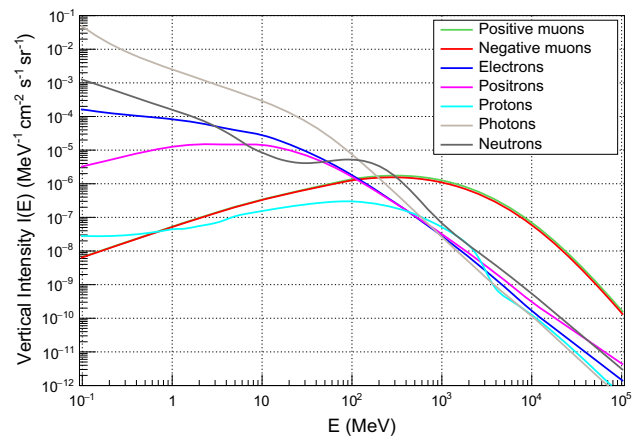


**Fig. 6** Differential vertical intensity of secondary cosmic rays at sea level as a function of the energy at (45° N 15° E) Earth Position and on August 1, 2018, computed using the PARMA model as described in the text. The contributions from the various particle species are plotted

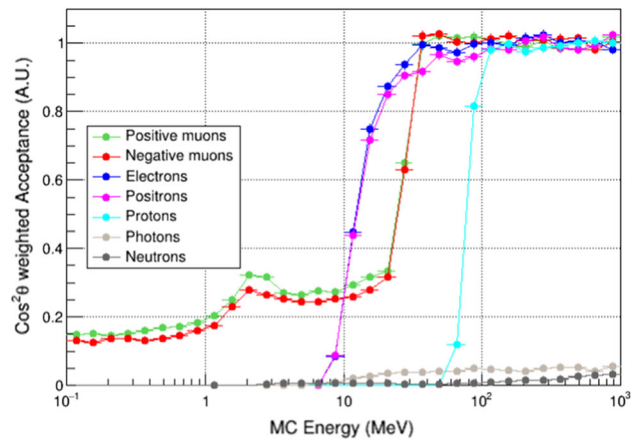


**Fig. 7** POLA detector acceptance weighted with  $\cos^2\theta$  and normalised to the unity above 500 MeV as a function of Monte Carlo (MC) energy. The coloured lines and markers refer to different particle types

**Table 2** Systematic uncertainties

Source	Magnitude of relative uncertainty
Pressure corrections	0.5%
Altitude	0.2% at 500 m
Inclination/Orientation	Negligible
Seasonal effect	0.25%
Daily fluctuations (for data at latitudes > 60°)	0.5%
Efficiency	0.4–0.7%
Material budget (except for Svalbard, Cosenza and Lampedusa)	1%
Total common systematic error	0.8–1.4%

<sup>1</sup> The public version of the PARMA code is available at the link <http://phits.jaea.go.jp/expacs/>.

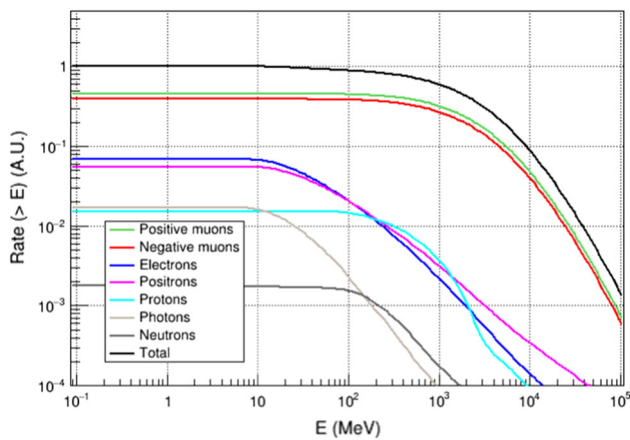


**Fig. 8** Expected integrated rate as a function of the minimum energy of secondary cosmic rays, for a point at sea level at (45° N 15° E) Earth Position, on August 1, 2018. For each kind of particle, the rate is normalised to the total rate (black line) at the lowest energy value. The coloured lines show the rates normalised in this way for different particles

generated, from 100 keV to 1 GeV.<sup>2</sup> We assumed a constant acceptance value for energies above 1 GeV. The simulation includes an adequate representation of the POLA detector in terms of material budget, comprising the external box, the scintillator tiles and their wrapping layers inside the box.

The detector acceptance, weighted with the  $\cos^2 \theta$  factor cited above, is shown in Fig. 7, as a function of energy. The acceptance reaches a plateau above about roughly 50 MeV for muons, electrons (positrons), and above 100 MeV for protons. The different values for the onset of the plateau depend on the different energy losses in the materials traversed by the various particle types. Photons and neutrons show a negligible contribution to the detector acceptance, since they have to interact in the detector or in the materials surrounding it, and produce charged particles to be actually revealed. It should be also noted that  $\mu^\pm$  of energy lower than few tens of MeV may decay inside the detector box, and the low energy daughter  $e^\pm$  are sometimes able to cross the scintillator planes and be detected. This is at the origin of the peak around 2 MeV of the corresponding acceptance curves.

The rates due to the various particle types expected in the POLA detectors are shown in Fig. 8, as a function of the particle energy. These rates were computed by folding the vertical cosmic ray differential flux shown in Fig. 6 (referred to the position 45°N 15°E, and day August 1, 2018) with the detector acceptance, and assuming a  $\cos^2 \theta$  angular dependence of the secondary cosmic rays at sea level, as it was done for Fig. 7. To better distinguish the various contributions, the rates shown in Fig. 8 were normalised to the total expected rate at the lowest energy value, shown as well. As it can be

<sup>2</sup> The public version of the FLUKA code is available at the link <http://www.fluka.org/fluka.php>.

seen, muons contribute to the total rate by about 85%, while electrons/positrons by about 12%.

In order to evaluate the dependence of the expected rate as a function of the latitude, the calculations described above have been repeated in the range from 20° N to 90° N. Results will be compared with experimental data in Sect. 6.

As a counter-check, we have also evaluated this rate by scaling the differential vertical intensity with a  $p \cos \theta$  factor ( $p$  being the momentum of the particle considered), and weighted the acceptance with  $\cos^3 \theta$  [17]. We find a slightly higher overall rate, by about 6%, with respect to the  $\cos^2 \theta$  approach discussed above. Nevertheless, no change occurs in the rate dependence as a function of the geographical latitude.

## 6 Results

The rate measured by the POLA-01 detector as a function of the geographical latitude, after all corrections outlined in Sect. 3 were applied, is shown in the top panel of Fig. 9. Note that, with respect to the results shown in [1], the measured rates presented here are corrected also by detector efficiency and seasonal effect, which were needless to consider in [1]; moreover, they are referred to the atmospheric pressure of 1012 mbar, as described in Sect. 3. The error bars shown in Fig. 9 include the statistical uncertainties, in black, and total uncertainties (i.e. statistical and systematic, summed in quadrature), in grey. From the measured data, it is possible to infer an increase in the cosmic particle rate with increasing latitude, until an almost flat plateau of the cosmic ray rate appears at latitudes above  $\approx 50^\circ$  N, as expected.

The cosmic particle rate measured by POLA-01 is shown in the bottom panel of Fig. 9, as a function of the vertical geomagnetic cutoff  $R$  (in units of GV). This was evaluated, for the various locations of interest here, using the International Geomagnetic Reference Field, version 13 (IGRF-13) [18]. Figure 9 data were fitted with the function suggested in [19]:

$$r(R) = r_0(1 - e^{-\alpha R^{-k}}) \quad (1)$$

where  $r$  is the rate as a function of the cutoff rigidity  $R$  and  $r_0$ ,  $\alpha$  and  $k$  are fit parameters found to be  $(35.15 \pm 0.05)$  Hz,  $(6.8 \pm 1.1)$  and  $(0.45 \pm 0.08)$ , respectively. The best fit function is shown in Fig. 9 as a blue line superimposed to the experimental data.

The expected rate evaluated from the simulation, following the procedure outlined in Sect. 5, is also shown in Fig. 10, normalised to the plateau data. The expectations are shown with a  $\pm 1\%$  light blue band, that reflects the peak-to-peak fluctuations observed in the data for latitudes above 60°N. The simulated rate shows a plateau starting from about 45°N

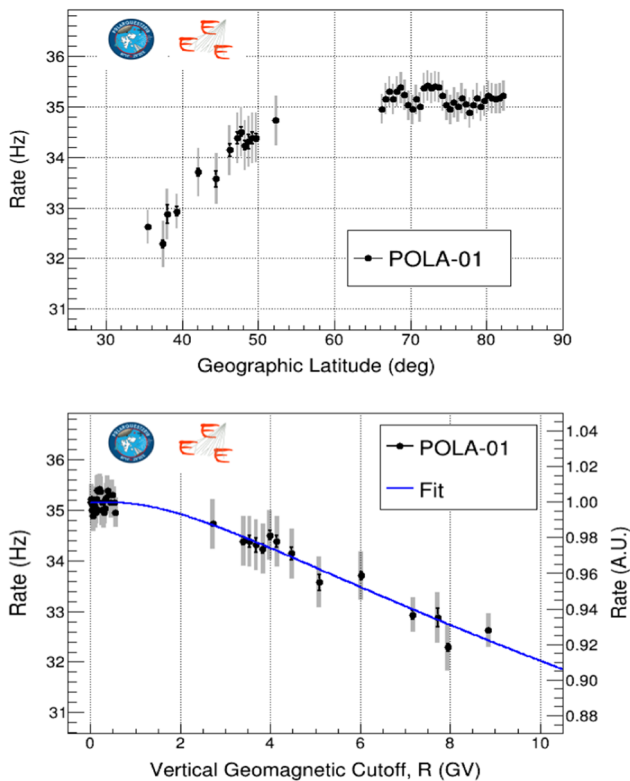


**Fig. 9** Cosmic particle rate measured by the POLA-01 detector as a function of the geographic latitude (top panel), and as a function of the vertical geomagnetic cutoff (bottom panel)

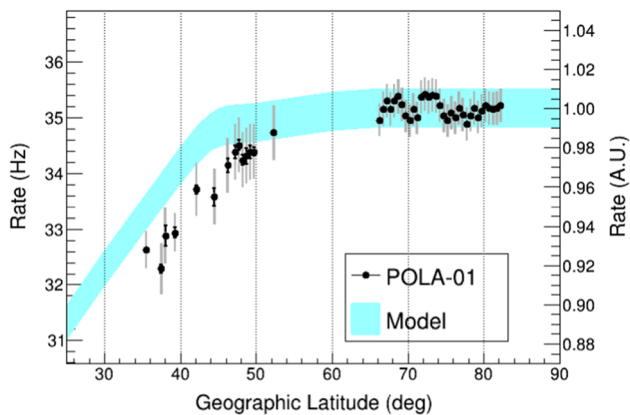


**Fig. 10** Cosmic particle rate measured by the POLA-01 detector as a function of the geographic latitude compared with the expectations of the PARMA model (light blue band)

in latitude (knee), that it is slightly earlier with respect to the one observed in the experimental data.

It is worth noting that the slope of the simulated rate, below the knee, is in good agreement with the experimental one.

Possible reasons for discrepancies between experimental data and simulations may arise, in the PARMA model, from the cosmic ray spectra at the top of the atmosphere, the solar modulation parameter, the density and composition profile

of the Earth atmosphere, the geomagnetic field model and finally the secondary cosmic ray yield at sea level.

It should also be reminded that the experimental data reported in this paper cover an energy region also extending much below the reference data used to tune the simulation spectra. Moreover, the uncertainties in the definition of the materials around the POLA-01 detector at the different locations during the data taking campaign (for instance, on the boat, the detector was placed on the deck and enclosed in an external plastic hutch, while, on the road, it was placed either close to buildings or in full open air, sometimes inside a car) can affect the simulated rate. Solar activity and specific environmental Earth conditions may introduce further uncertainties in the PARMA output.

However, an evaluation of the various contributions of these uncertainties did not indicate any significant effect on the latitude dependence of the estimated rate but rather an overall scale factor. This is the reason why, in Fig. 10, we have normalised the simulated rate to the experimentally measured rate above 60° N latitude.

The energy spectra of the galactic cosmic rays used in the PARMA code were taken from [20]. More recent experimental results are available, obtained, among others, by the AMS-02 [21], CALET [22] and DAMPE [23] collaborations, which led to an updated cosmic ray flux. The use of a more recent proton flux and solar modulation could improve the agreement between model prediction and PolarquEEEst data. Also, other models are available in literature, which could be used to compute the secondary cosmic ray flux at sea level (see for instance [24]). A comparison among the various models would give interesting insights on the topic. However, this is beyond the scope of the present paper and will be addressed in a forthcoming paper.

In spite of the above considerations, the simulation reported here reproduces reasonably well the measured data. It should also be noticed that the possibility of a normalisation to a plateau value represents a unique feature of the PolarquEEEst data, thanks to the large set of measurements available at latitudes above 60° N. This offers an important constraint to the parameterisation of the simulation codes.

## 7 Conclusions

The PolarquEEEst experiment measured the cosmic particle rate at sea level in the latitude interval 35°–82° N. The data, after corrections, show an increase of the rate with latitude, until a flattening above 50° N appears due to the geomagnetic field effect. The measurements provide for the first time a set of consistent, systematic and precise results in this extended region, spanning over nearly 50° of latitude, well beyond the Polar Arctic Circle. When compared with a widely used analytical model for radiation in the atmosphere (PARMA), our

results show a substantial agreement, within the experimental uncertainties and the uncertainty of the model predictions, thus providing useful constraints for the simulation.

With the goal to better complement these studies, in July 2019 three POLA detectors were installed permanently at Ny Ålesund, in the Spitsbergen island of the Svalbard archipelago, to allow a new precision, long term measurement and monitoring of cosmic ray fluxes at these extreme latitudes.

**Acknowledgements** We would like to thank P. Catapano and P. Galinelli, respectively project leader and skipper of the Polarquest2018 expedition. We also thank the students and teachers of the high schools involved in preparing the detectors and in monitoring POLA-02 and POLA-03 operation during the whole data taking period.

**Data availability statement** This manuscript has no associated data or the data will not be deposited. [Authors' comment: The datasets generated during the current study are available in the EEE webpage, <https://eee.centrofermi.it/images/Data/dataLatFin.txt>.]

**Open Access** This article is licensed under a Creative Commons Attribution 4.0 International License, which permits use, sharing, adaptation, distribution and reproduction in any medium or format, as long as you give appropriate credit to the original author(s) and the source, provide a link to the Creative Commons licence, and indicate if changes were made. The images or other third party material in this article are included in the article's Creative Commons licence, unless indicated otherwise in a credit line to the material. If material is not included in the article's Creative Commons licence and your intended use is not permitted by statutory regulation or exceeds the permitted use, you will need to obtain permission directly from the copyright holder. To view a copy of this licence, visit <http://creativecommons.org/licenses/by/4.0/>.

Funded by SCOAP<sup>3</sup>. SCOAP<sup>3</sup> supports the goals of the International Year of Basic Sciences for Sustainable Development.

## References

1. M. Abbrescia et al., New high precision measurements of the cosmic charged particle rate beyond the Arctic Circle with the PolarquEEEst experiment. *Eur. Phys. J. C* **80**(7), 665 (2020) [Erratum: *Phys. J. C* **80**(9): 897 (2020)]
2. A.H. Compton, A geographic study of cosmic rays. *Phys. Rev.* **43**, 387 (1933)
3. G. Lemaître, M.S. Vallarta, On Compton's latitude effect of cosmic radiation. *Phys. Rev.* **43**, 87 (1933)
4. R. Pyle, P. Evenson, J.W. Bieber, J.M. Clem, J.E. Humble, M.L. Duldig, The use of <sup>3</sup>He tubes in a neutron monitor latitude survey, in *Proceedings 26th International Cosmic Ray Conference (Salt Lake City, UT, August 17–25, 1999)*, vol. 7 (1999), p. 386
5. L. Dorman, *Cosmic Rays in Magnetospheres of the Earth and Other Planets, Volume 358 of Astrophysics and Space Science Library* (Springer, Berlin, 2009)
6. J.P. Saraiva, A. Blanco, J.A. Garzón, D. García-Castro, L. Lopes, V. Villasante-Marcos, The TRISTAN detector—2018–2019 latitude survey of cosmic rays. *JINST* **15**(09), C09024 (2020)
7. Polarstern Project at DESY, [https://www.desy.de/school/school\\_lab/zeuthen\\_site/cosmic\\_particles/experiments/polarstern\\_project/index\\_eng.html](https://www.desy.de/school/school_lab/zeuthen_site/cosmic_particles/experiments/polarstern_project/index_eng.html)
8. T. Sato, Analytical model for estimating terrestrial cosmic ray fluxes nearly anytime and anywhere in the world: extension of PARMA/EXPACS. *PLoS One* **10**(12), e0144679 (2015)
9. T. Sato, Analytical model for estimating the zenith angle dependence of terrestrial cosmic ray fluxes. *PLoS One* **11**(8), e0160390 (2016)
10. EEE Collaboration, <https://eee.centrofermi.it/en/>
11. A. Zichichi, Progetto EEE — Extreme Energy Events - La Scienza nelle Scuole. Società Italiana di Fisica, 2017. [https://eee.centrofermi.it/images/EEE-PaperAZ/EEE\\_Paper\\_AZ-2017.pdf](https://eee.centrofermi.it/images/EEE-PaperAZ/EEE_Paper_AZ-2017.pdf)
12. PolarQuest expedition, <http://www.polarquest2018.org/>
13. R.R.S. Mendonça et al., The temperature effect in secondary cosmic rays (muons) observed at the ground: analysis of the Global Muon Detector Network data. *ApJ* **830**, 88 (2016)
14. P.A. Zyla et al., Review of particle physics. *PTEP* **2020**(8), 083C01, 2020 and 2021 update
15. A. Ferrari, P.R. Sala, A. Fassò, J. Ranft, FLUKA: a multi-particle transport code (program version 2005). CERN Yellow Report CERN-2005-010, SLAC-R-773, INFN-TC-05-11 (2005)
16. T.T. Böhlen, F. Cerutti, M.P.W. Chin, A. Fassò, A. Ferrari, P.G. Ortega, A. Mairani, P.R. Sala, G. Smirnov, V. Vlachoudis, The FLUKA code: developments and challenges for high energy and medical applications. *Nucl. Data Sheets* **120**, 211 (2014)
17. D. Reyna, A simple parameterization of the cosmic-ray muon momentum spectra at the surface as a function of zenith angle. [arXiv:hep-ph/0604145v2](https://arxiv.org/abs/hep-ph/0604145v2)
18. P. Alken, E. Thébault, C.D. Beggan, H. Amit, J. Aubert, J. Baerenzung, T.N. Bondar, W.J. Brown, S. Califf, A. Chambodut et al., International geomagnetic reference field: the thirteenth generation. *Earth Planets Space* **73**(1), 1 (2021)
19. L.I. Dorman, S.G. Fedchenko, L.V. Granitsky, G.A. Rishe, Coupling and barometer coefficients for measurements of cosmic ray variations at altitudes of 260–400 mb, in *Proceedings 11th International Cosmic Ray Conference (Budapest, August 25–September 4, 1969)*, volume 29 suppl. 2 of *Acta Physica Academic Science Hungary* (1970), p. 233
20. Daniel Matthiä, Thomas Berger, Alankrita I. Mrigakshi, Gänther. Reitz, A ready-to-use galactic cosmic ray model. *Adv. Space Res.* **51**(3), 329–338 (2013)
21. M. Aguilar et al., Precision measurement of the proton flux in primary cosmic rays from rigidity 1 GV to 1.8 TV with the alpha magnetic spectrometer on the International Space Station. *Phys. Rev. Lett.* **114**, 171103 (2015)
22. O. Adriani et al., Direct measurement of the cosmic-ray proton spectrum from 50 GeV to 10 TeV with the Calorimetric Electron Telescope on the International Space Station. *Phys. Rev. Lett.* **122**(18), 181102 (2019)
23. Q. An et al., Measurement of the cosmic-ray proton spectrum from 40 GeV to 100 TeV with the DAMPE satellite. *Sci. Adv.* **5**(9), eaax3793 (2019)
24. Christian Sarmiento-Cano, Mauricio Suárez-Durán, Rolando Calderón-Ardila, Adriana Vásquez-Ramírez, Andrei Jaimes-Motta, Luis A. Núñez, Sergio Dasso, Iván. Sidelnik, Hernán Asorey, The ARTI framework: cosmic rays atmospheric background simulations. *Eur. Phys. J. C* **82**(11), 1019 (2022)